Homoleptic Mesityl Complexes of Cobalt(II). Synthesis, Crystal Structure, and Theoretical Description of Bis(μ-mesityl)dimesityldicobalt

Klaus H. Theopold,*[1b] Jerome Silvestre,[1a] Erin K. Byrne,[1b] and Darrin S. Richeson[1b]

Department of Chemistry, Baker Laboratory, Cornell University, Ithaca, New York 14853, and Institut de Recherches sur la Catalyse, CNRS, LP 5401, Laboratoire de Chimie Theorique, 2, AV. A. Einstein, 62626 Villeurbanne Cedex, France

Received January 23, 1989

The previously prepared complex $[Li(THF)_4]^+[Co(mesityl)_3]^-$ was characterized by spectroscopic techniques and magnetic measurements. Protonation of this complex yielded the dimeric $(\mu\text{-mesityl})_2[Co(mesityl)]_2$. The crystal structure of this dimer was determined by X-ray diffraction. It crystallized in the triclinic space group $P\bar{1}$ with a = 12.598 (3) Å, b = 16.046 (8) Å, c = 16.855 (6) Å, α = 67.63 (4)°, β = 87.85 (4)°, γ = 84.65 (4)°, and Z = 4. One of the two independent molecules in the asymmetric unit exhibited a short distance between a cobalt atom and an ortho methyl group of a bridging mesityl ligand. Spectroscopic methods were used to rule out an agostic M–H–C interaction as the source of this proximity. A partial deuteriation experiment revealed an unusually large deuterium isotope effect on the ^1H chemical shifts of the dimer. The magnetic susceptibility of the title compound was measured in the temperature range 2–280 K. Extended Hückel molecular orbital calculations suggested the presence of a metal–metal bond.

Introduction

Our interest in stabilizing unusually high formal oxidation states of cobalt has led us to investigate homoleptic alkyl complexes of this metal with bulky alkyl ligands.[2] The mesityl (2,4,6-trimethylphenyl) group is a sterically demanding moiety, which is known to form stable organometallic compounds.[3] Herein we report the synthesis and characterization of a dimeric cobalt(II) mesityl complex and an unusual phenomenon discovered in ^1H NMR spectra of partially deuteriated analogues.

The reaction of cobalt halides with mesityl anions has some history. As early as 1961 Tsutsui and Zeiss claimed the isolation of dimesitylcobalt from a mixture of cobaltous chloride and mesitylmagnesium bromide.[4] They did not characterize the reaction product, however. A more recent reinvestigation of this system by Seidel and Bürger[5] showed that the products of this reaction were actually anionic complexes containing both mesityl and bromide ligands in varying proportions. The latter authors also reported the isolation of $LiCo(mes)_3 \cdot 4THF$ from a reaction of $CoCl_2$ with excess mesityllithium. This material was characterized by measurement of its room temperature magnetic moment, reaction with $HgCl_2$ to give (mesityl)HgCl, elemental analysis, and GC analysis of the volatile hydrolysis products. $LiCo(mes)_3 \cdot 4THF$ provided the starting point for our work, and we will begin with a more detailed description of its synthesis and spectroscopic characterization.

Scheme I

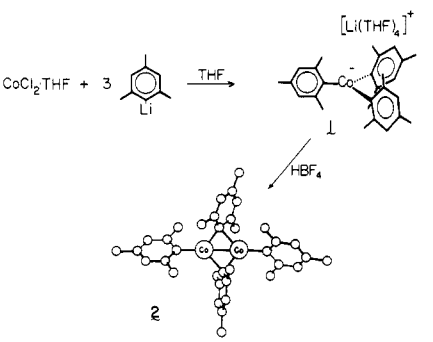

Results and Discussion

Addition of 0.3 equiv of $CoCl_2 \cdot THF$ to a cold (−78 °C) solution of mesityllithium in THF and subsequent warming to room temperature gave a light green solution. Removal of the solvent and treatment of the solid residue with Et_2O yielded a green oil, which upon cooling solidified to green crystals of $[Li(THF)_4]^+[Co(mes)_3]^-$ (1) in 75% yield (Scheme I). Once crystalline, this compound was insoluble in nonpolar solvents like toluene or Et_2O but very soluble in THF. The ^1H NMR spectrum of a THF-d_8 solution of 1 at room temperature exhibited resonances consistent with one type of mesityl group and resonances for free THF (due to exchange of the coordinated THF by THF-d_8). The chemical shifts of the mesityl resonances were temperature-dependent. A plot of the chemical shifts versus $1/T$ was linear (Figure 1) as expected for a paramagnetic substance obeying the Curie law.[6] The molar magnetic susceptibility of 1 in the temperature interval 4–300 K was measured with a Faraday balance and showed Curie behavior. The effective magnetic moment of 3.8 μ_B at 300 K was consistent with the three unpaired electrons expected for a high-spin d^7 ion in a trigonal ligand envi-

(1) (a) Institut de Recherches sur la Catalyse, CNRS, France. (b) Cornell University.

(2) (a) Byrne, E. K.; Richeson, D. S.; Theopold, K. H. *J. Chem. Soc., Chem. Commun.* **1986**, 1491. (b) Byrne, E. K.; Theopold, K. H. *J. Am. Chem. Soc.* **1987**, *109*, 1282. (c) Byrne, E. K.; Theopold, K. H. *J. Am. Chem. Soc.*, in press.

(3) (a) Machelett, B. *Z. Chem.* **1976**, *16*, 116. (b) Glowiak, T.; Grobelny, R.; Jezowska-Trzebiatowska, B.; Kreisel, G.; Seidel, W.; Uhlig, E. *J. Organomet. Chem.* **1978**, *155*, 39. (c) Lattermann, K.-J.; Seidel, W. *Z. Chem.* **1983**, *23*, 445. (d) Seidel, W.; Kreisel, G. *Z. Chem.* **1982**, *22*, 113. (e) Seidel, W.; Kreisel, G. *Z. Anorg. Allg. Chem.* **1988**, *559*, 118. (f) Sharp, P. R.; Astruc, D.; Schrock, R. R. *J. Organomet. Chem.* **1979**, *182*, 477. (g) Gambarotta, S.; Floriani, C.; Chiesi-Villa, A.; Guastini, C. *J. Chem. Soc., Chem. Commun.* **1983**, 1087, 1128, 1156, 1304; **1984**, 886. (h) Bartlett, R. A.; Olmstead, M. M.; Power, P. P.; Shoner, S. C. *Organometallics* **1988**, *7*, 1801.

(4) Tsutsui, M.; Zeiss, H. *J. Am. Chem. Soc.* **1961**, *83*, 825.

(5) Seidel, W.; Burger, I. *Z. Chem.* **1977**, *17*, 31.

(6) Bertini, I.; Luchinat, C. *NMR of Paramagnetic Molecules in Biological Systems*; Benjamin/Cummings: Menlo Park, CA, 1986; p 44.

0276-7333/89/2308-2001$01.50/0

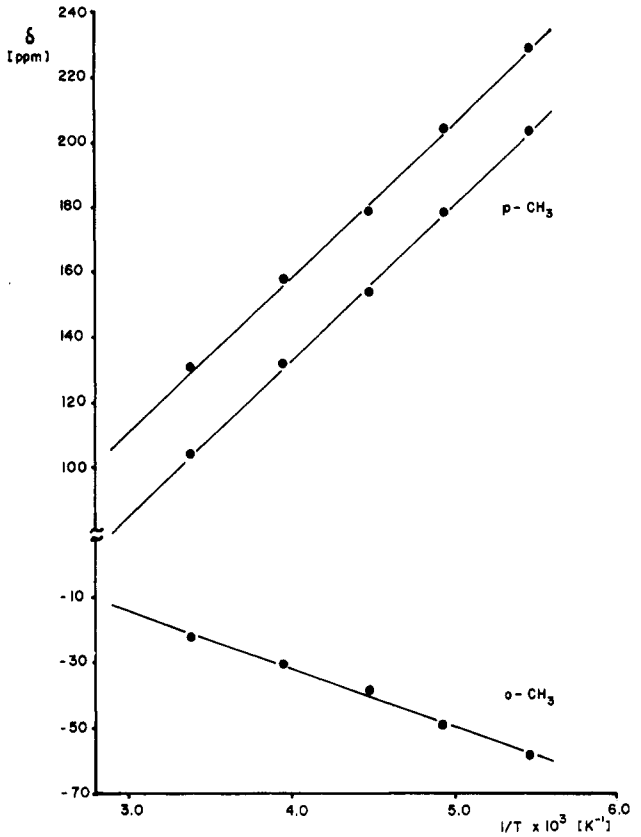

Figure 1. Plot of the chemical shifts of the mesityl groups of 1 versus $1/T$.

ronment.[7] Reaction of 1 with 1 equiv of PPN^+Cl^- (PPN = bis(triphenylphosphine)nitrogen(1+) resulted in exchange of the $Li(THF)_4$ counterion and formation of $PPN^+[Co(mes)_3]^-$. This substitution did not affect the chemical shifts of the mesityl groups or the color of the compound. The above observations indicate a merely electrostatic interaction between the $[Co(mes)_3]^-$ fragment and the lithium ion. Apparently the mesityl group is bulky enough to stabilize three coordinate cobalt, similar to the recently reported $[Li(THF)_4]^+[Mn(mes)_3]^-$.[3h]

When 1.0 equiv of $HBF_4 \cdot Et_2O$ was added to a cold (−30 °C) solution of 1 in THF, the color of the solution immediately changed from light green to a dark green. Evaporation of the solvent, extraction with pentane, and recrystallization of the material so obtained from pentane yielded black crystals. The ^1H NMR spectrum of this new compound (2) exhibited resonances consistent with two inequivalent mesityl groups (Figure 4a). In solution 2 decomposed slowly at room temperature and rapidly when exposed to air.

The structure of 2 was determined by X-ray diffraction at low temperature. Suitable crystals were grown by cooling of a pentane solution of 2 to −35 °C (see Table IV for details). The asymmetric unit contains two independent molecules with slightly different bond distances and angles. Figure 2 shows computer generated drawings of both dimers with the atom numbering scheme.

Selected bond distances and interatomic angles are compiled in Table II. The individual molecules possess no crystallographic symmetry. Each cobalt is bound to one terminal and two bridging mesityl groups. Such bridging aryl ligands are well precedented in the organometallic

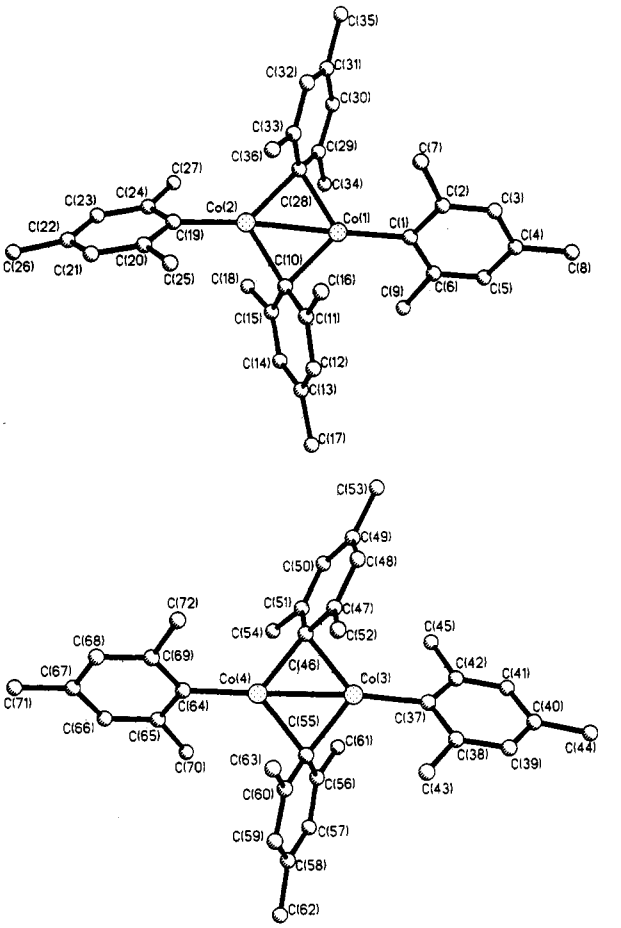

Figure 2. The two crystallographically independent molecules of 2 with the atom numbering scheme. See Table II for interatomic distances and angles.

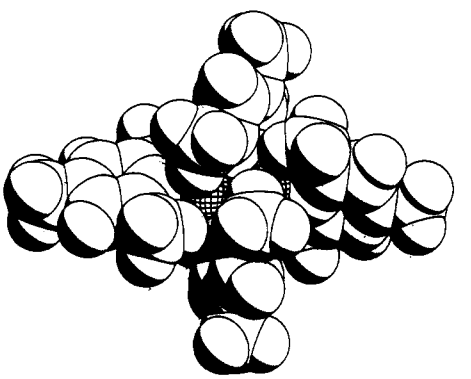

Figure 3. Space-filling representation of 2 (van der Waals radii: H (1.2), C (1.6), Co (1.7)).

chemistry of both main group and transition elements.[8] The Co–Co distances of 2.512 (2) and 2.519 (2) Å are certainly indicative of metal–metal bonding, despite the presence of unpaired electrons in 2. Each local CoC_3 coordination environment is very close to planar, with the sum of the C–Co–C angles being 360.0° (Co1), 359.9° (Co2), 359.3 (Co3), and 359.5 (Co4), respectively. The overall

(7) (a) Hope, H.; Olmstead, M. M.; Murray, B. D.; Power, P. P. *J. Am. Chem. Soc.* **1985**, *107*, 712. (b) Cotton, F. A.; Wilkinson, G. *Advanced Inorganic Chemistry*, 4th ed.; Wiley: New York, 1980; pp 625–629.

(8) (a) Malone, J. F.; McDonald, W. S. *J. Chem. Soc., Dalton Trans.* **1972**, 2646. (b) Malone, J. F.; McDonald, W. S. *J. Chem. Soc., Dalton Trans.* **1972**, 2649. (c) Thoennes, D.; Weiss, E. *Chem. Ber.* **1978**, *111*, 3726. (d) ten Hoedt, R. W. M.; Noltes, J. G.; van Koten, G.; Spek, A. L. *J. Chem. Soc., Dalton Trans.* **1978**, 1800. (e) Bradford, C. W.; Nyholm, R. S.; Gainsford, G. J.; Guss, J. M.; Ireland, P. R.; Mason, R. *J. Chem. Soc., Chem. Commun.* **1972**, 87. (f) Gambarotta, S.; Floriani, C.; Chiesi-Villa, A.; Guastini, C. *J. Chem. Soc., Chem. Commun.* **1983**, 1087, 1128, 1156, 1304.

Table I. Atomic Coordinates (×10⁴) and Equivalent Isotropic Displacement Coefficients (Å² × 10⁴) for 2

	x	y	z	U(eq), Å²		x	y	z	U(eq), Å²
Co(1)	1530 (1)	4831 (1)	6992 (1)	263 (3)	Co(3)	3464 (1)	-275 (1)	1951 (1)	261 (3)
Co(2)	2006 (1)	6179 (1)	7273 (1)	258 (3)	Co(4)	3206 (1)	980 (1)	2510 (1)	286 (3)
C(1)	1287 (5)	3729 (4)	6775 (4)	264 (23)	C(37)	3704 (5)	-1341 (4)	1618 (4)	279 (23)
C(2)	2096 (5)	3291 (4)	6442 (4)	274 (23)	C(38)	4686 (5)	-1886 (4)	1802 (4)	275 (23)
C(3)	1948 (5)	2488 (4)	6336 (4)	321 (26)	C(39)	4836 (6)	-2668 (4)	1631 (4)	327 (25)
C(4)	1014 (5)	2091 (4)	6550 (4)	299 (24)	C(40)	4030 (6)	-2962 (5)	1300 (4)	334 (26)
C(5)	197 (5)	2511 (4)	6881 (4)	291 (24)	C(41)	3074 (6)	-2449 (5)	1123 (4)	369 (27)
C(6)	325 (5)	3304 (4)	6999 (4)	279 (24)	C(42)	2898 (5)	-1648 (4)	1281 (4)	291 (24)
C(7)	3168 (5)	3687 (5)	6171 (5)	378 (29)	C(43)	5592 (5)	-1618 (5)	2195 (4)	357 (27)
C(8)	869 (7)	1220 (5)	6426 (5)	501 (34)	C(44)	4214 (7)	-3835 (5)	1136 (5)	546 (35)
C(9)	-579 (5)	3709 (5)	7397 (5)	365 (28)	C(45)	1816 (6)	-1110 (5)	1064 (5)	423 (30)
C(10)	1134 (5)	5167 (4)	8031 (4)	272 (23)	C(46)	2726 (5)	1003 (4)	1380 (4)	288 (24)
C(11)	1515 (5)	4324 (4)	8666 (4)	281 (24)	C(47)	3355 (5)	1084 (4)	640 (4)	311 (25)
C(12)	880 (6)	3870 (5)	9355 (4)	370 (27)	C(48)	2876 (6)	1273 (4)	-147 (4)	355 (26)
C(13)	-142 (6)	4218 (5)	9440 (5)	395 (30)	C(49)	1788 (5)	1397 (4)	-244 (4)	345 (26)
C(14)	-522 (5)	5054 (5)	8844 (4)	347 (28)	C(50)	1165 (5)	1360 (4)	471 (4)	337 (26)
C(15)	95 (5)	5534 (4)	8151 (4)	308 (25)	C(51)	1599 (5)	1159 (4)	1261 (4)	331 (25)
C(16)	2636 (6)	3909 (4)	8613 (5)	393 (28)	C(52)	4559 (5)	1030 (5)	672 (4)	386 (28)
C(17)	-830 (7)	3680 (6)	10181 (5)	564 (36)	C(53)	1275 (7)	1599 (6)	-1101 (5)	513 (33)
C(18)	-328 (6)	6459 (5)	7562 (5)	429 (30)	C(54)	870 (6)	1120 (5)	2007 (5)	426 (30)
C(19)	2322 (5)	7186 (4)	7609 (4)	305 (26)	C(55)	3738 (5)	-354 (4)	3156 (4)	295 (25)
C(20)	2891 (5)	7016 (5)	8373 (4)	338 (27)	C(56)	3084 (5)	-996 (4)	3726 (4)	262 (23)
C(21)	2938 (6)	7675 (5)	8708 (5)	381 (29)	C(57)	3390 (5)	-1486 (4)	4564 (4)	297 (25)
C(22)	2434 (6)	8536 (5)	8312 (5)	445 (33)	C(58)	4323 (5)	-1356 (4)	4893 (4)	312 (25)
C(23)	1939 (5)	8725 (4)	7543 (5)	391 (29)	C(59)	4954 (5)	-721 (5)	4346 (4)	321 (26)
C(24)	1862 (5)	8073 (4)	7183 (5)	356 (27)	C(60)	4699 (5)	-242 (4)	3493 (4)	298 (25)
C(25)	3451 (6)	6079 (5)	8855 (4)	407 (29)	C(61)	2045 (6)	-1168 (5)	3419 (5)	446 (30)
C(26)	2429 (7)	9242 (6)	8708 (6)	619 (41)	C(62)	4637 (6)	-1910 (5)	5809 (4)	477 (31)
C(27)	1284 (7)	8335 (5)	6348 (5)	525 (33)	C(63)	5480 (6)	382 (5)	2923 (5)	434 (31)
C(28)	2316 (5)	5884 (4)	6206 (4)	244 (23)	C(64)	3005 (5)	1992 (4)	2911 (4)	320 (26)
C(29)	1665 (5)	6136 (4)	5461 (4)	305 (24)	C(65)	2554 (6)	1882 (5)	3714 (4)	363 (28)
C(30)	2120 (6)	6310 (4)	4660 (4)	313 (25)	C(66)	2452 (6)	2602 (5)	4007 (5)	424 (32)
C(31)	3211 (5)	6306 (4)	4544 (4)	283 (24)	C(67)	2782 (6)	3438 (5)	3510 (5)	433 (32)
C(32)	3845 (5)	6079 (4)	5256 (4)	307 (25)	C(68)	3219 (6)	3552 (5)	2712 (5)	422 (31)
C(33)	3432 (5)	5864 (4)	6073 (4)	283 (24)	C(69)	3334 (6)	2857 (4)	2411 (5)	361 (27)
C(34)	449 (5)	6191 (5)	5530 (4)	437 (30)	C(70)	2188 (7)	988 (5)	4285 (4)	483 (32)
C(35)	3693 (6)	6528 (5)	3661 (4)	487 (32)	C(71)	2687 (7)	4201 (6)	3840 (6)	638 (43)
C(36)	4195 (5)	5571 (5)	6832 (4)	352 (27)	C(72)	3801 (7)	3028 (5)	1525 (5)	526 (33)

[a] Equivalent isotropic U defined as one-third of the trace of the orthogonalized U_{ij} tensor.

Co_2C_4 cores of the molecules deviate slightly from planarity, adopting butterfly geometries with dihedral angles between the CoC_3 planes of 174.7° (dimer I) and 174.9° (dimer II). **2** is closely related structurally to several dinuclear cobalt amides and alkoxides, which Power et al. have characterized by X-ray diffraction.[9] Among these it resembles most closely the amides, which also feature close Co···Co contacts (ca. 2.57 Å) and coplanar Co_2N_4 cores. The terminal mesityl groups are staggered with respect to each other (average angle = 81°). The bridging aryl rings are twisted out of the expected orientation perpendicular to the Co–Co vector, such that the average angle between the ring planes is 45°. This particular arrangement is probably a consequence of the extreme steric congestion suffered by the ortho methyl groups of **2**, as depicted in Figure 3. It also leads to some unusually short nonbonded distances between cobalt atoms and some of the ortho methyl groups of the mesityl bridges. The shortest of these (Co3–C52) measures only 2.79 Å. We were intrigued by the possibility that this short contact might reflect an agostic Co–H–C interaction[10] between the extremely electron-deficient cobalt[11] and the nearby alkyl group. Floriani et al. have recently determined the structures of two molecules generated by the activation of C–H bonds of the methyl groups of mesityl ligands bridging two zirconium atoms.[12]

A number of spectroscopic criteria have been used for the identification of agostic alkyls.[10] The increased C–H bond length sometimes leads to the observation of a lowered stretching frequency in the region of ca. 2700–2350 cm^{-1}. The IR spectrum of **2** shows no such absorption. The partial metal hydride character of the bridging hydrogen atom frequently results in a high-field shift of the averaged ^1H NMR signal of a methyl or methylene group involved in an agostic interaction. Whereas at least one of the ortho methyl resonances of **2** appears at very high field (-20.7 ppm at room temperature in toluene-d_8), this shift is more likely a consequence of the paramagnetic nature of the compound, thus rendering the criterion useless in our case. Another common result of the weakened C–H bond in a three-center M–H–C bridge is a lowered ^{13}C–H coupling constant. The resonances of **2** are sharp enough to determine these values from the ^{13}C satellites in the ^1H NMR spectrum. At 119.6 and 122.1 Hz for the two ortho methyl resonances, respectively, they provide no evidence for any unusual bonding situation.

Having exhausted these straightforward methods of analysis, we decided to perform a partial deuteriation experiment in order to remove any remaining doubts. This method was developed by Shapley et al. for the characterization of $[Os_3(CO)_{10}(CH_3)H]$.[13] It depends on an

(9) (a) Murray, B. D.; Power, P. P. *Inorg. Chem.* **1984**, *23*, 4584. (b) Hope, H.; Olmstead, M. M.; Murray, B. D.; Power, P. P. *J. Am. Chem. Soc.* **1985**, *107*, 712. (c) Olstead, M. M.; Power, P. P.; Sigel, G. *Inorg. Chem.* **1986**, *25*, 1027.

(10) Brookhart, M.; Green, M. L. H. *J. Organomet. Chem.* **1983**, *250*, 395.

(11) Counting the bridging mesityl ligands as one-electron donors, each cobalt obtains an 11-electron configuration.

(12) Stella, S.; Chiang, M.; Floriani, C. *J. Chem. Soc., Chem. Commun.* **1987**, 161.

Table II. Interatomic Distances (Å) and Angles (deg) for 2

Bond Distances

Co(1)–Co(2)	2.512 (2)	Co(1)–C(1)	1.989 (7)	Co(3)–C(37)	1.988 (7)	Co(3)–C(46)	2.052 (6)
Co(1)–C(10)	2.052 (7)	Co(1)–C(28)	2.026 (6)	Co(3)–C(47)	2.442 (6)	Co(3)–C(55)	2.028 (7)
Co(2)–C(10)	2.031 (6)	Co(2)–C(19)	1.981 (8)	Co(4)–C(46)	2.005 (7)	Co(4)–C(55)	2.056 (6)
Co(2)–C(28)	2.042 (7)	C(1)–C(2)	1.404 (10)	Co(4)–C(64)	1.977 (8)	C(37)–C(38)	1.418 (9)
C(1)–C(6)	1.413 (9)	C(2)–C(3)	1.395 (11)	C(37)–C(42)	1.395 (10)	C(38)–C(39)	1.386 (11)
C(2)–C(7)	1.526 (9)	C(3)–C(4)	1.362 (10)	C(38)–C(43)	1.514 (10)	C(39)–C(40)	1.377 (11)
C(4)–C(5)	1.392 (10)	C(4)–C(8)	1.517 (12)	C(40)–C(41)	1.368 (10)	C(40)–C(44)	1.522 (12)
C(5)–C(6)	1.386 (11)	C(6)–C(9)	1.518 (10)	C(41)–C(42)	1.405 (11)	C(42)–C(45)	1.523 (9)
C(10)–C(11)	1.421 (8)	C(10)–C(15)	1.424 (9)	C(46)–C(47)	1.422 (9)	C(46)–C(51)	1.428 (9)
C(11)–C(12)	1.384 (9)	C(11)–C(16)	1.519 (9)	C(47)–C(48)	1.392 (10)	C(47)–C(52)	1.512 (9)
C(12)–C(13)	1.379 (10)	C(13)–C(14)	1.387 (9)	C(48)–C(49)	1.374 (10)	C(49)–C(50)	1.398 (10)
C(13)–C(17)	1.516 (10)	C(14)–C(15)	1.386 (9)	C(49)–C(53)	1.511 (11)	C(50)–C(51)	1.368 (10)
C(15)–C(18)	1.498 (9)	C(19)–C(20)	1.418 (10)	C(51)–C(54)	1.512 (10)	C(55)–C(56)	1.417 (8)
C(19)–C(24)	1.405 (8)	C(20)–C(21)	1.381 (12)	C(55)–C(60)	1.410 (10)	C(56)–C(57)	1.379 (8)
C(20)–C(25)	1.528 (9)	C(21)–C(22)	1.388 (10)	C(56)–C(61)	1.512 (10)	C(57)–C(58)	1.384 (10)
C(22)–C(23)	1.375 (12)	C(22)–C(26)	1.518 (15)	C(58)–C(59)	1.379 (9)	C(58)–C(62)	1.505 (9)
C(23)–C(24)	1.406 (12)	C(24)–C(27)	1.503 (11)	C(59)–C(60)	1.381 (9)	C(60)–C(63)	1.508 (9)
C(28)–C(29)	1.431 (9)	C(28)–C(33)	1.414 (9)	C(64)–C(65)	1.401 (10)	C(64)–C(69)	1.414 (9)
C(29)–C(30)	1.384 (9)	C(29)–C(34)	1.529 (9)	C(65)C(66)	1.413 (13)	C(65)–C(70)	1.495 (10)
C(30)–C(31)	1.380 (10)	C(31)–C(32)	1.377 (9)	C(66)–C(67)	1.377 (10)	C(67)–C(68)	1.386 (12)
C(31)–C(35)	1.509 (10)	C(32)–C(33)	1.379 (9)	C(67)–C(71)	1.519 (15)	C(68)–C(69)	1.384 (13)
C(33)–C(36)	1.528 (9)	Co(3)–Co(4)	2.519 (2)	C(69)–C(72)	1.519 (11)		

Bond Angles

Co(2)–Co(1)–C(1)	175.0 (2)	Co(2)–Co(1)–C(10)	51.6 (2)	C(37)–Co(3)–C(47)	108.0 (2)	C(46)–Co(3)–C(47)	35.6 (2)
C(1)–Co(1)–C(10)	130.4 (2)	Co(2)–Co(1)–C(28)	52.2 (2)	Co(4)–Co(3)–C(55)	52.4 (2)	C(37)–Co(3)–C(55)	122.4 (2)
C(1)–Co(1)–C(28)	125.9 (3)	C(10)–Co(1)–C(28)	103.7 (3)	C(46)–Co(3)–C(55)	102.6 (3)	C(47)–Co(3)–C(55)	127.1 (3)
Co(1)–Co(2)–C(10)	52.4 (2)	Co(1)–Co(2)–C(19)	174.4 (2)	Co(3)–Co(4)–C(46)	52.4 (2)	Co(3)–Co(4)–C(55)	51.4 (2)
C(10)–Co(2)–C(19)	122.0 (3)	Co(1)–Co(2)–C(28)	51.6 (2)	C(46)–Co(4)–C(55)	103.2 (3)	Co(3)–Co(4)–C(64)	178.2 (2)
C(10)–Co(2)–C(28)	103.9 (3)	C(19)–Co(2)–C(28)	134.0 (3)	C(46)–Co(4)–C(64)	126.0 (2)	C(55)–Co(4)–C(64)	130.3 (3)
Co(1)–C(1)–C(2)	121.4 (5)	Co(1)–C(1)–C(6)	122.4 (5)	Co(3)–C(37)–C(38)	120.6 (5)	Co(3)–C(37)–C(42)	122.5 (5)
C(2)–C(1)–C(6)	116.0 (6)	C(1)–C(2)–C(3)	121.6 (6)	C(38)–C(37)–C(42)	116.5 (6)	C(37)–C(38)–C(39)	121.2 (6)
C(1)–C(2)–C(7)	120.8 (6)	C(3)–C(2)–C(7)	117.6 (6)	C(37)–C(38)–C(43)	119.9 (6)	C(39)–C(38)–C(43)	118.9 (6)
C(2)–C(3)–C(4)	121.7 (7)	C(3)–C(4)–C(5)	118.0 (7)	C(38)–C(39)–C(40)	121.5 (6)	C(39)–C(40)–C(41)	118.2 (7)
C(3)–C(4)–C(8)	120.9 (7)	C(5)–C(4)–C(8)	121.2 (6)	C(39)–C(40)–C(44)	120.2 (6)	C(41)–C(40)–C(44)	121.6 (7)
C(4)–C(5)–C(6)	121.5 (6)	C(1)–C(6)–C(5)	121.3 (6)	C(40)–C(41)–C(42)	121.8 (7)	C(37)–C(42)–C(41)	120.8 (6)
C(1)–C(6)–C(9)	119.7 (7)	C(5)–C(6)–C(9)	119.0 (6)	C(37)–C(42)–C(45)	120.4 (7)	C(41)–C(42)–C(45)	118.8 (7)
Co(1)–C(10)–Co(2)	75.9 (2)	Co(1)–C(10)–C(11)	96.3 (5)	Co(3)–C(46)–Co(4)	76.8 (2)	Co(3)–C(46)–C(47)	87.4 (4)
Co(2)–C(10)–C(11)	127.6 (5)	Co(1)–C(10)–C(15)	122.6 (5)	Co(4)–C(46)–C(47)	128.0 (5)	Co(3)–C(46)–C(51)	121.8 (5)
Co(2)–C(10)–C(15)	109.6 (4)	C(11)–C(10)–C(15)	117.4 (5)	Co(4)–C(46)–C(51)	113.7 (5)	C(47)–C(46)–C(51)	116.6 (6)
C(10)–C(11)–C(12)	120.8 (6)	C(10)–C(11)–C(16)	120.8 (5)	Co(3)–C(47)–C(46)	57.1 (3)	Co(3)–C(47)–C(48)	131.4 (5)
C(12)–C(11)–C(16)	118.4 (5)	C(11)–C(12)–C(13)	120.9 (5)	C(46)–C(47)–C(48)	120.7 (6)	Co(3)–C(47)–C(52)	86.6 (3)
C(12)–C(13)–C(14)	119.5 (6)	C(12)–C(13)–C(17)	119.3 (6)	C(46)–C(47)–C(52)	121.0 (6)	C(48)–C(47)–C(52)	118.2 (6)
C(14)–C(13)–C(17)	121.2 (7)	C(13)–C(14)–C(15)	121.3 (6)	C(47)–C(48)–C(49)	121.8 (6)	C(48)–C(49)–C(50)	117.9 (7)
C(10)–C(15)–C(14)	120.1 (5)	C(10)–C(15)–C(18)	120.9 (5)	C(48)–C(49)–C(53)	121.4 (6)	C(50)–C(49)–C(53)	120.7 (6)
C(14)–C(15)–C(18)	118.9 (6)	Co(2)–C(19)–C(20)	120.8 (5)	C(49)–C(50)–C(51)	122.4 (6)	C(46)–C(51)–C(50)	120.5 (6)
Co(2)–C(19)–C(24)	121.9 (6)	Co(20)–C(19)–C(24)	116.6 (7)	C(46)–C(51)–C(54)	120.2 (6)	C(50)–C(51)–C(54)	119.2 (6)
C(19)–C(20)–C(21)	121.6 (6)	C(19)–C(20)–C(25)	119.9 (7)	Co(3)–C(55)–Co(4)	76.2 (2)	Co(3)–C(55)–C(56)	107.8 (5)
C(21)–C(20)–C(25)	118.5 (6)	C(20)–C(21)–C(22)	121.6 (7)	Co(4)–C(55)–C(56)	122.9 (5)	Co(3)–C(55)–C(60)	127.7 (5)
C(21)–C(22)–C(23)	117.2 (8)	C(21)–C(22)–C(26)	121.6 (8)	Co(4)–C(55)–C(60)	99.8 (5)	C(56)–C(55)–C(60)	116.7 (5)
C(23)–C(22)–C(26)	121.2 (7)	C(22)–C(23)C(24)	122.9 (6)	C(55)–C(56)–C(57)	120.8 (6)	C(55)–C(56)–C(61)	120.4 (5)
C(19)–C(24)–C(23)	119.8 (7)	C(19)–C(24)–C(27)	120.9 (7)	C(57)–C(56)–C(61)	118.8 (5)	C(56)–C(57)–C(58)	122.0 (6)
C(23)–C(24)–C(27)	119.3 (6)	Co(1)–C(28)–Co(2)	76.3 (2)	C(57)–C(58)–C(59)	117.5 (6)	C(57)–C(58)–C(62)	120.5 (6)
Co(1)–C(28)–C(29)	98.4 (4)	Co(2)–C(28)–C(29)	127.7 (5)	C(59)–C(58)–C(62)	122.0 (7)	C(58)–C(59)–C(60)	122.4 (7)
Co(1)–C(28)–C(33)	125.1 (4)	Co(2)–C(28)–C(33)	107.6 (5)	C(55)–C(60)–C(59)	120.5 (6)	C(55)–C(60)–C(63)	120.6 (6)
C(29)–C(28)–C(33)	116.6 (5)	C(28)–C(29)–C(30)	120.8 (6)	C(59)–C(60)–C(63)	118.8 (6)	Co(4)–C(64)–C(65)	121.7 (5)
C(28)–C(29)–C(34)	121.0 (6)	C(30)–C(29)–C(34)	118.2 (6)	Co(4)–C(64)–C(69)	121.6 (5)	C(65)–C(64)–C(69)	116.7 (7)
C(29)–C(30)–C(31)	121.4 (6)	C(30)–C(31)–C(32)	118.2 (6)	C(64)–C(65)–C(66)	121.1 (6)	C(64)–C(65)–C(70)	120.2 (7)
C(30)–C(31)–C(35)	120.7 (6)	C(32)–C(31)–C(35)	121.1 (6)	C(66)–C(65)–C(70)	118.7 (7)	C(65)–C(66)–C(67)	121.2 (7)
C(31)–C(32)–C(33)	122.6 (6)	C(28)–C(33)–C(32)	120.3 (6)	C(66)–C(67)–C(68)	117.9 (8)	C(66)–C(67)–C(71)	120.6 (8)
C(28)–C(33)–C(36)	120.5 (5)	C(32)–C(33)–C(36)	119.2 (6)	C(68)–C(67)–C(71)	121.5 (7)	C(67)–C(68)–C(69)	122.1 (7)
Co(4)–Co(3)–C(37)	174.8 (2)	Co(4)–Co(3)–C(46)	50.8 (2)	C(64)–C(69)–C(68)	121.0 (7)	C(64)–C(69)–C(72)	119.3 (7)
C(37)–Co(3)–C(46)	134.3 (3)	Co(4)–Co(3)–C(47)	77.1 (2)	C(68)–C(69)–C(72)	119.7 (6)		

equilibrium isotope effect, which favors the M–H–C bridged isomer of a partially deuterium-labeled methyl group interacting with a metal atom over the M–D–C bridged one. This disproportionate exposure of the H atom to the "metal hydride like" site in turn leads to an upfield shift of the average ^{1}H NMR resonance of the methyl group for every D atom introduced. Shifts in the range of 0.34–0.77 ppm per deuterium have been observed.[14]

Treatment of mesitylene with DMSO-d_6 and a small amount of sodium hydride yielded a sample of mesitylene, in which an average of 3.2 benzylic hydrogens had been replaced by deuterium as determined by ^{1}H NMR.[15] This was converted to mesityl bromide by reaction with bromine

(13) Calvert, R. B.; Shapley, J. R. *J. Am. Chem. Soc.* **1978**, *100*, 7726.

(14) Dawkins, D. M.; Green, M.; Orpen, A. G.; Stone, F. G. A. *J. Chem. Soc., Chem. Commun.* **1982**, 41. (b) Howarth, O. W.; McAteer, C. H.; Moore, P.; Morris, G. E. *J. Chem. Soc., Chem. Commun.* **1981**, 506. (c) Casey, C. P.; Fagan, P. J.; Miles, W. H. *J. Am. Chem. Soc.* **1982**, *104*, 1134.

(15) Chen, T.-S.; Wolinska-Mocydlarz, J.; Leitch, L. C. *J. Labelled Compd.* **1970**, *VI*, 285.

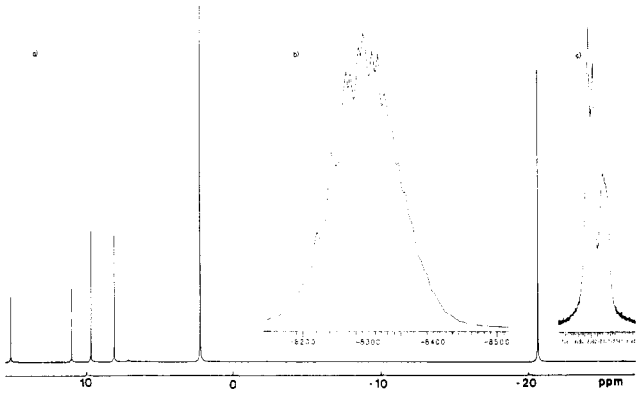

Figure 4. (a) Full ^1H NMR spectrum of **2** (toluene-d_8, 25 °C), (b) expanded view of the high-field resonance of **2**-$d_?$, and (c) expanded view of the high-field resonance of **2** prepared from a mixture of **1**-d_0 and **1**-d_9.

in CCl_4. Mass spectrometric analysis of the mesityl bromide indicated it to be a statistical mixture of molecules containing between zero and nine deuteria, with a maximum abundance of the d_3 species. Lithiation with ^{t}BuLi and reaction with $CoCl_2$·THF yielded a sample of **1**-$d_?$.[16] The ^1H NMR spectrum of this material to our surprise exhibited three resonances for the para methyl groups of the mesityl ligands at δ 104.3, 103.9, and 103.4 ppm, whereas the ortho methyl resonance appeared unchanged. This effect might have been anticipated, however, because Horn and Everett[17] some time ago reported the observation of separate ^1H NMR resonances for the CH_3, CH_2D, and CHD_2 groups of partially deuteriated tris(2,4-pentanedionato)vanadium(III). They interpreted the large differences in chemical shifts (ca. 0.5 ppm) as intrinsic isotope effects amplified by the large isotropic shift caused by the paramagnetism of the molecule.

While the above observation might make the interpretation of the partial deuteriation experiment ambiguous when applied to a paramagnetic molecule, we were curious enough to proceed. Protonation of **1**-$d_?$ in the usual fashion yielded a sample of **2**-$d_?$. The ^1H NMR spectrum of this material provided another surprise. The ortho methyl resonance at −20.7 ppm, which had been a sharp singlet in the unlabeled material, now appeared as a complex multiplet of approximately 20 partially resolved spectral lines (Figure 4b). The full width of this multiplet measured ca. 0.5 ppm, independent of the field strength of the spectrometer (90–400 MHz). The overall appearance of the signals did not change dramatically upon cooling the sample to −40 °C, despite some shifts in individual peaks. These results rule out coupling as the origin of the splitting and are most readily explained with the presence of a large number (at least 20) of different methyl groups. This is possible in principle due to the presence of mesityl groups of various levels and patterns of deuteriation, although such an explanation would invoke an unprecedented intrinsic deuterium isotope effect on the chemical shift of a proton operating over six and possibly more bonds.[18] In other words, the chemical shift of, e.g., a CH_2D group must be affected in a measurable way by the number and/or positions of deuterium atoms in the methyl groups meta to it or even those in another mesityl ligand of the same molecule.

Scheme II

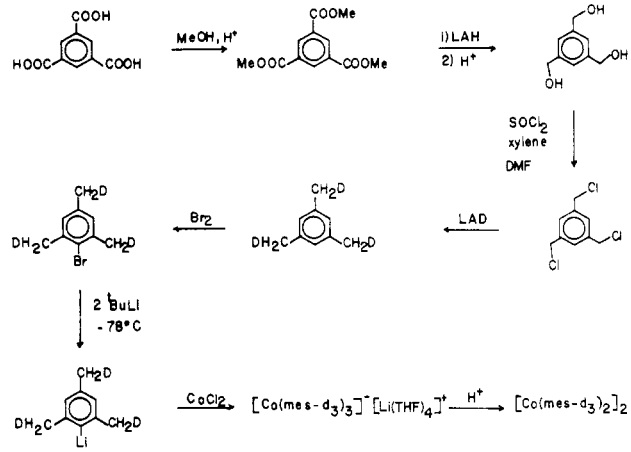

We felt it worth while to address this last point by modifying the experiment. Starting with 1,3,5-benzenetricarboxylic acid and following the route outlined in Scheme II, we prepared a sample of specifically labeled mesityl-d_3 bromide. Lithiation and reaction with $CoCl_2$·THF yielded **1**-d_9. The ^1H NMR spectrum of this compound exhibited singlets for all three mesityl resonances, consistent with the presence of CH_2D groups only. Furthermore, protonation of **1**-d_9 with 1 equiv of HBF_4 yielded **2**-d_{12}, displaying a simple spectrum consisting of the expected six singlets. However, when a 1:1 mixture of **1**-d_0 and **1**-d_9 was treated in the same manner the ^1H NMR spectrum of the isolated **2** exhibited the high-field multiplet shown in Figure 4c. At least three resonances were clearly resolved, and the presence of a fourth (shoulder on most upfield peak) seemed indicated. Since this mixture contained only two types of mesityl groups (d_0 and d_3), the chemical shifts of the CH_3 and CH_2D groups responsible for the high-field resonances were affected by the identity of the other mesityl ligands within the same molecule. The detection of more than two resonances thus points to an isotope effect on the chemical shift operating between different mesityl groups; i.e., the chemical shift of the ortho methyl groups of one aryl ligand of **2** depends in a measurable way on whether the methyl groups of another such aryl ligand contain a deuterium atom or not.

What is the origin of these isotope induced shifts? Clearly the paramagnetism of the molecule serves to magnify shift differences, which would be too small to be detected in a diamagnetic molecule. Horn and Everett[17] showed that the contact contribution to the isotropic shift may be responsible for the relatively large shift differences between methyl groups of different deuterium contents. However, the dipolar shift with its sensitive dependence on the position of the resonating nucleus with respect to the molecular axes[19] may also be responsible for the long-range effect described above. It is well-known that C–D bonds are shorter than comparable C–H bonds.[20] If the geometrical structure of **2** indeed reflects severe nonbonded interactions between the ortho-methyl groups (see Figure 3), any relief of this strain by substituting a smaller deuterium for a proton may lead to a perturbation of the molecular structure large enough to be detectable in the

(16) The subscript ? indicates the heterogeneity of mixtures of molecules containing several mesityl groups, each of which may contain between 0 and 9 deuteria.
(17) Horn, R. R.; Everett, G. W., Jr. *J. Am. Chem. Soc.* **1971**, *93*, 7173.
(18) Hansen, P. E. *Annu. Rep. NMR Spectrosc.* **1983**, *15*, 105.
(19) Reference 6, pp 36–38.
(20) (a) Bartell, L. S.; Kuchitsu, K.; DeNeui, R. J. *J. Chem. Phys.* **1961**, *35*, 1211. (b) Laurie, V. W.; Herschbach, D. R. *J. Chem. Phys.* **1962**, *37*, 1687. (c) Bartell, L. S.; Higginbotham, H. K. *J. Chem. Phys.* **1965**, *42*, 851. (9) Wollrab, J. L. *Rotational Spectra and Molecular Structure*; Academic Press: New York, 1967; p 110.

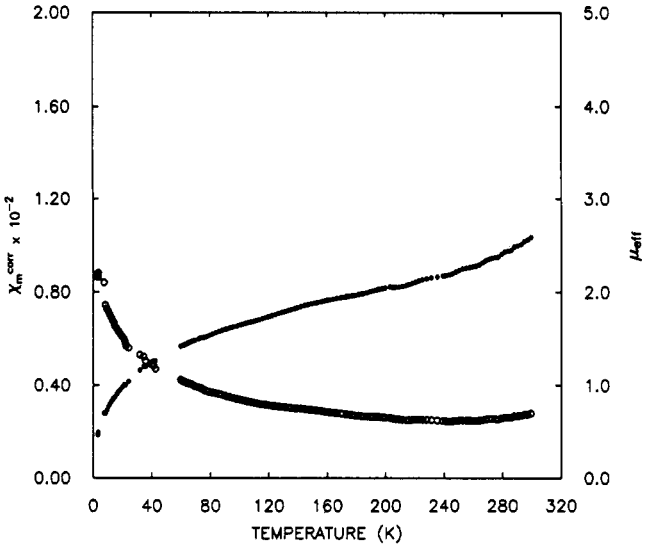

Figure 5. Temperature dependence of the molar magnetic susceptibility (open circles) and the effective magnetic moment (filled circles) of **2** (corrected for diamagnetism).

NMR spectrum. Finally, there seems to be no reason to invoke an agostic interaction to explain the spectroscopic data. On the basis of the available evidence, we believe that **2** does not engage in such bonding. If nothing else, this serves to point out that the availability of empty valence orbitals on the metal coupled with proximity of an alkyl group are not sufficient conditions for formation of an M–H–C bridge.

Turning now to the question of metal–metal bonding in **2**, we note that metal–metal distance is not a failsafe criterion for establishing such bonding.[21] We have employed magnetic measurements and EHMO calculations to elucidate the electronic structure of **2**. Figure 5 depicts the temperature dependence of its molar magnetic susceptibility and effective magnetic moment. At first glance the temperature dependence of μ_{eff} would seem to indicate antiferromagnetic coupling between two $S = {}^3/_2$ nuclei. The complex clearly possesses a singlet ground state. The small rise in the susceptibility at low temperatures (<40 K) and the nonzero intercept of μ_{eff} may be attributed to the superimposed Curie–Weiss behavior of a small amount of a paramagnetic impurity. However, the susceptibility shows a peculiar temperature dependence, and all attempts to fit the data with an expression derived from the HDVV model[22] failed. The magnitude and the apparent lack of temperature dependence of the susceptibility imply a large temperature-independent paramagnetic term in the susceptibility. Temperature-independent paramagnetism (TIP) results from mixing of thermally inaccessible excited states with the ground state.[23] Its magnitude is inversely proportional to the difference in energy between the ground and excited states. In the presence of an inhomogeneous magnetic field such mixing lowers the energy of the ground state and results in an attraction of the sample into areas of higher field strength. The effect is a temperature independent and positive susceptibility. Extended Hückel calculations (see below) indicate that **2** exhibits metal–metal bonding and that the three highest

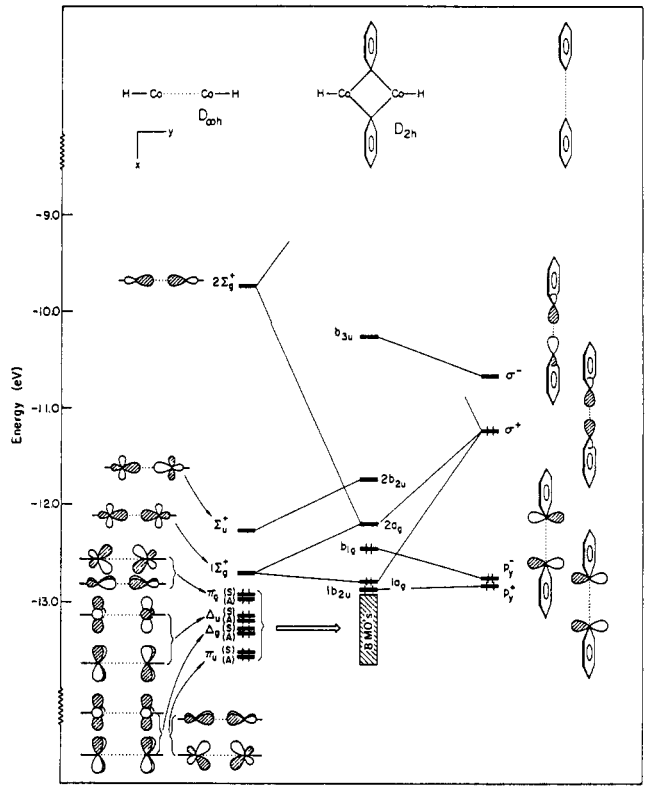

Figure 6. Orbital structure of an idealized model for dimer **2**.

Scheme III

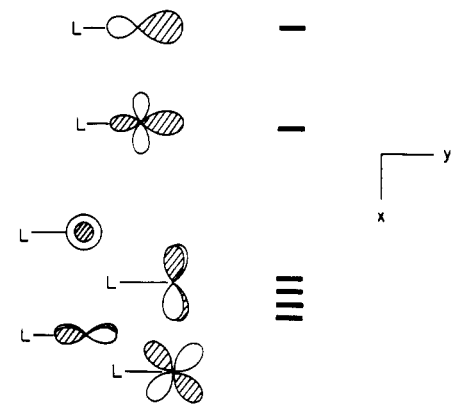

occupied molecular orbitals of the dimer lie close in energy to an empty metal–metal bonding orbital. The resulting availability of low-lying excited ligand field states could give rise to the large TIP term that contributes to the unusual behavior of the susceptibility of **2**. A TIP term of the magnitude observed in this system would require an energy gap between the ground and exited states of **2** on the order of 1000 cm^{-1}.[24] We cannot rule out the possibility that the slight rise of the susceptibility at higher temperatures (>240 K) represents the onset of thermal population of spin states of higher multiplicity characteristic of antiferromagnetic coupling. However, this effect may also be caused by decomposition of **2**.

To gain a better understanding of the bonding in **2**, we have probed its electronic structure by means of extended Hückel calculations.[25] The relevant computational and geometrical details are gathered in the Experimental Section. A simple, yet informative approach to the orbital

(21) Richeson, D. S.; Hsu, S.-W.; Fredd, N. H.; VanDuyne, G.; Theopold, K. H. *J. Am. Chem. Soc.* **1986**, *108*, 8273.
(22) (a) Martin, R. L. In *New Pathways in Inorganic Chemistry*; Ebsworth, Maddock, Sharp, Eds.; Cambridge University: Cambridge, 1968; Chapter 9. (b) Cairns, C. J.; Busch, Daryle, H. *Coord. Chem. Rev.* **1986**, *69*, 1.
(23) Figgis, B. N. *Introduction to Ligand Fields*; Wiley: New York, 1966; p 253.
(24) Carlin, R. L. *Magnetochemistry*; Springer: Berlin, 1986; p 12.
(25) (a) Hoffmann, R. *J. Chem. Phys.* **1963**, *69*, 1397. (b) Hoffmann, R.; Lipscomb, W. N. *J. Chem. Phys.* **1962**, *36*, 3179, 3289; **1962**, *37*, 2872.

Scheme IV

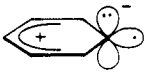

structure of the cobalt dimer makes use of the conceptual fragmentation shown at the top of Figure 6. The left fragment (H–Co···Co–H) features a set of valence orbitals which are readily constructed as the in-phase and out-of-phase combinations of the valence orbitals of two M–L units. The important levels are schematically depicted in Scheme III: above a group of d-centered states (z^2, xy, xz, and yz in the coordinate system specified) one finds $x^2 - y^2$, destabilized by σ-antibonding with the ligand donor function and a sixth MO, mainly sp in character. A calculation on the dimeric fragment showed its valence orbitals to be ordered as indicated on the left of Figure 6.[26] The fragment has $D_{\infty h}$ symmetry, and the levels are labeled accordingly.[27] In order to increasing energy we encounter four sets of degenerate states—π-bonding, δ-bonding, δ-antibonding, and π-antibonding—followed by the bonding $x^2 - y^2$ combination, its antibonding counterpart, and still higher the symmetric combination of the sp hybrids. The right-hand side of the figure shows the four levels of the bridging aryl groups which interact strongly with the bimetallic core. They are two σ lone-pair combinations (σ^+, σ^-) and two MO's labeled p_y^- and p_y^+. These are the symmetric components of the 1e sets of the aromatic π-system. Thus, each bridging phenyl is viewed as in Scheme IV, with two electrons in the p orbital of the ipso carbon and one electron in the σ-hybrid. Given this electronic configuration the organic fragment takes the form of a neutral biradical and the σ^+ MO is its HOMO while σ^- acts as an acceptor. Within this formalism the bimetallic fragment is neutral and the eight lowest MO's are filled. The molecular orbital of the model for dimer **2** are shown in the middle of Figure 6. They were derived following the usual perturbation rules: molecular orbitals mix if they evolve with the same symmetry properties under the D_{2h} point group of the idealized Co dimer. $\Pi_g(A)$, $\Delta_u(A)$, $\Pi_u(A)$, and $\Delta_g(A)$ are not affected by interaction with the biphenyl fragment, since these MO's do not match in symmetry any orbitals of the (Ph···Ph) unit. These four orbitals enter the block labeled "eight MO's". The remaining four MO's in this block are the in-phase combinations generated by mixing of $\Delta_g(S)$, $\Delta_u(S)$, $\Pi_g(S)$, and $\Pi_u(S)$ with σ^+, p_y^+, p_y^-, and σ^-, respectively. Besides being Co–C bonding, some of these combinations generate an appreciable amount of Co–Co bonding (see below). $1b_{2u}$ is the middle level resulting from the threefold mixing of Σ_u^+, $\Delta_u(S)$, and p_y^+ and is essentially Co–C nonbonding. Next in energy is 1_{ag}, primarily $1\Sigma_g^+$ (85% in our computations) mixed with σ^+, along with minor contributions from $\Delta_g(S)$ and $2\Sigma_g^+$. In the diamagnetic ground state b_{1g} (the antibonding combination of p_y^- and $\Pi_g(S)$) is the HOMO. Just a little higher in energy is 2_{ag}, the antibonding counterpart of 1_{ag}, but maintained very low in energy by second-order mixing with $2\Sigma_g^+$: the magnitude of this mixing is large due to the enormous overlap between $2\Sigma_g^+$ and σ^+ (0.3836). The two highest levels are 2_{bu} and b_{3u}, deriving from antibonding interactions within the pairs (Σ_u^+, p_y^-) and ($\Pi_u(S)$, σ^-), respectively.

Several observations can be made given the orbital structure of the dimer and the topology of its constituent

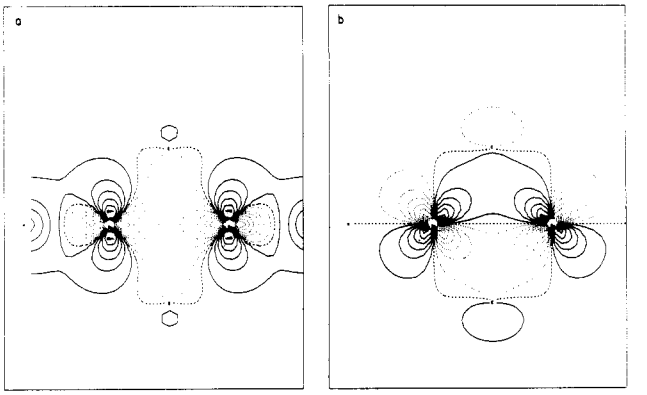

Figure 7. (a) Contour plot of $1a_g$ MO in the xy plane, (b) contour plot of the bonding combination of σ^- and $\Pi_u(S)$. The contours plotted are ±0.4, ±0.3, ±0.2, ±0.125, ±0.075, ±0.025, and 0.0. Solid lines represent nonzero values. Dashed lines are nodes.

Table III. Co–Co Overlap Population for Various MO Occupations

configuration	Co–Co overlap pop.
$1b_{2u}^2 1a_g^2 b_{1g}^2$	0.1090
$1b_{2u}^2 1a_g^2 b_{1g}^1 2a_g^1$	0.1330
$1b_{2u}^2 1a_g^1 b_{1g}^1 2a_g^1 2b_{2u}^1$	0.1150
$1b_{2u}^1 1a_g^1 b_{1g}^1 2a_g^1 2b_{2u}^1 b_{3u}^1$	0.1170

MO's. The small energy differences between the five orbitals clustered around the HOMO (i.e. $1b_{2u}$, $1a_g$, b_{1g}, 2_{ag}, and $2b_{2u}$) are consistent with the experimental observation of a large temperature-independent paramagnetism.

The complex appears to be metal–metal bonded. The main contribution to the bonding is made by orbital 1_{ag}, which descends from $1\Sigma_g^+$. A good measure of the Co–Co bonding is the overlap population computed for that bond. In the singlet configuration, it is 0.110. For comparison, the Co–Co overlap population is 0.140 for $Co_2(CO)_8$[28] at the same Co–Co distance (our calculation). Figure 7a shows the contours of molecular orbital 1_{ag} in the xy plane, displaying the σ-bonding character of the wave function. Another contribution to Co–Co bonding results from through-bond coupling.[29] This is shown in Figure 7b. In the bonding combination between σ^- and $\Pi_u(S)$ (one of the "eight MO's"), some π-bonding remains between the metal atoms as a byproduct of the Co–C bonding. This interaction provides 0.021 of the total Co–Co overlap population.

A remarkable feature of the electronic structure of the dimer is the suggestion that electronic excitation to higher spin states will *not* necessarily decrease the extent of metal–metal bonding. Note that b_{1g} is metal–metal antibonding. Promotion of an electron from this orbital into 2_{ag} should increase Co–Co bonding. Table III lists the Co–Co overlap populations computed for different MO occupations.

Conclusions

The mesityl group stabilizes highly electron-deficient homoleptic aryl complexes of cobalt(II) with the unusually low coordination number 3. A dimer of the elusive dimesitylcobalt was prepared and structurally characterized. It contained mesityl groups bridging two cobalt atoms. A short distance between a cobalt atom and an ortho methyl group was attributed to severe steric interactions between mesityl ligands rather than to an agostic M–H–C bond.

(26) Calculations were also performed with R = phenyl; the π levels of the terminal phenyl groups slightly complicate the overall picture but do not alter the conclusions drawn here for R = H.

(27) Cotton, F. A. *Chemical Applications of Group Theory*; 2nd ed.; Wiley-Interscience: New York, 1971.

(28) Summer, G. G.; Klug, H. P.; Alexander, L. F. *Acta Crystallogr.* **1964**, *17*, 732.

(29) Hoffmann, R. *Acc. Chem. Res.* **1971**, *4*, 1.

Partial deuteriation experiments carried out in this context revealed an unusually large deuterium isotope effect on the proton chemical shifts of this paramagnetic molecule. Magnetic measurements showed a large temperature-independent paramagnetism and EHMO calculations indicated significant metal–metal bonding in the dimer.

Experimental Section

General Comments. ^{1}H NMR spectra were recorded at 25 °C (unless indicated otherwise) on a Varian EM 390, XL 200, XL 400, or Bruker WM 300 spectrometer. IR spectra were obtained on a Perkin-Elmer 337 spectrometer. Gas chromatographic analyses were carried out on a Hewlett-Packard 5890 gas chromatograph equipped with an HP 3390 A integrator using a 6 ft × $^1/_8$ in. stainless-steel column packed with 3% OV 17 on Supelcoport 80/100. All manipulations involving air-sensitive organometallic compounds were carried out in a Vacuum Atmosphere inert-atmosphere box under N_2 or on a Schlenk line using Ar. Solvents were distilled under N_2 from purple benzophenone ketyl. Cobaltous chloride was dried by heating in vacuo. $CoCl_2$·THF was prepared by Soxhlet extraction of dry $CoCl_2$ with THF. Mesityl bromide was stored over activated molecular sieves. HBF_4·Et_2O was used as received and stored under N_2 at −35 °C.

$[Li(THF)_4]^+[Co(mesityl)_3]^-$ (1). A 1.9 M solution (25.0 mL) of ^{t}BuLi in pentane (47.5 mmol) was added dropwise to a cold (−78 °C) solution of 5.00 g of mesityl bromide (25.1 mmol) in ca. 200 mL of THF (note: the specified order of addition was crucial). After the addition was complete, the solution was warmed until the white precipitate dissolved and cooled back down to −78 °C. $CoCl_2$·THF (1.50 g, 7.2 mmol) was added as a solid and the suspension slowly warmed to room temperature under stirring. The solution eventually assumed a light green color. The solvent was removed under reduced pressure and the flask transferred into the drybox. Treatment of the solid residue with Et_2O yielded a green oil, which was immiscible with Et_2O but could be forced through a glass frit. Cooling of the Et_2O/oil mixture to −35 °C induced the oil to crystallize. Light green crystals of **1** were isolated (3.87 g, 76% yield). ^{1}H NMR (THF-d_8): 130.0 (s, 2 H), 103.3 (s, 3 H), 3.58 (m, THF), 1.75 (m, THF), −20.6 (br s, 6 H) ppm. IR (Nujol): 1580 (w), 1250 (w), 1205 (w), 1040 (s), 912 (w), 885 (m), 840 (m), 706 (w) cm^{-1}.

$[PPN]^+[Co(mesityl)_3]^-$. A solution of 225 mg of **1** (0.316 mmol) in 5 mL of THF was added to a suspension of PPN^+Cl^- (PPN = bis(triphenylphosphine)nitrogen(1+), $[Ph_3P{=}N{=}PPh_3]^+$) (190 mg, 0.331 mmol) in 15 mL of THF. The solution was filtered and evaporated to dryness and the residue recrystallized from THF/Et_2O at −35 °C. Yellow green crystals of $[PPN]^+[Co(mesityl)_3]^-$ (235 mg) were isolated (78% yield). ^{1}H NMR (THF-d_8): 131.5 (s, 6 H), 103.5 (s, 9 H), 9.92 (s, 18 H), 9.21 (s, 12 H), −19.6 (br s, 18 H) ppm. IR (Nujol): 3030 (w), 1580 (w), 1435 (s), 1290 (m), 1275 (s), 1260 (m), 1200 (w), 1170 (w), 1152 (w), 1107 (s), 1016 (w), 990 (m), 836 (m), 790 (w), 750 (m), 741 (m), 719 (s), 686 (s), 545 (m), 530 (w) cm^{-1}.

(μ-Mesityl)$_2$[Co(mesityl)]$_2$ (2). A solution of 180 mg of HBF_4·Et_2O (1.11 mmol) in 4 mL of Et_2O was added all at once to a cold (−30 °C) solution of 800 mg of **1** (1.12 mmol) in 15 mL of THF. The color of the solution immediately changed to dark green. After the solution was warmed to room temperature, the solvent was removed under vacuum and the solid residue extracted with Et_2O. Recrystallization from Et_2O at −30 °C yielded 180 mg of **2** in the form of black crystals (54% yield). ^{1}H NMR (C_6D_6): 15.2 (s, 2 H), 10.9 (s, 2 H), 9.5 (s, 3 H), 8.0 (s, 3 H), 2.2 (s, 6 H), −20.7 (s, 6 H) ppm. IR (Nujol): 1580 (m), 1270 (m), 1015 (w), 840 (m), 700 (w) cm^{-1}. Anal. Calcd for $C_{36}H_{44}Co_2$: C, 72.72; H, 7.46. Found: C, 73.01; H, 7.56. **2** (22 mg, 0.037 mmol) was dissolved in 1.5 mL of Et_2O and 10 μL of toluene (0.094 mmol) added as internal standard. To this solution was added an excess of HBF_4·Et_2O, and the resulting colorless solution was filtered through alumina. Quantitative GC analysis indicated the liberation of 0.142 mmol of mesitylene.

Mesityl-d_7 Bromide.[16] Mesitylene (6 mL) was exchanged once following the procedure by Chen et al.[15] using 5 g of DMSO-d_6 (99%) and 500 mg of sodium hydride. ^{1}H NMR ($CDCl_3$): 6.85 (s, 3 H), 2.32 (br s, 5.8 H) ppm. IR (neat): 2980 (s), 2895 (s), 2150 (br, w), 1600 (s), 1450 (m), 1260 (w), 1030 (br, w), 790 (br, m), 678 (br, m) cm^{-1}. This was converted to mesityl-d_7 bromide following Smith's *Organic Syntheses* procedure.[30] ^{1}H NMR ($CDCl_3$): 6.88 (s), 2.365 (s, *o*-CH_3), 2.349 (t, J_{HD} = 2.3 Hz, *o*-CH_2D), 2.333 (q, J_{HD} = 2.2 Hz, *o*-CHD_2), 2.229 (s, *p*-CH_3), 2.214 (t, J_{HD} = 2.3 Hz, *p*-CH_2D), 2.197 (q, J_{HD} = 2.2 Hz, *p*-CHD_2) ppm. IR (neat): 2990 (w), 2890 (m), 2150 (br, w), 1575 (m), 1450 (m), 1430 (m), 1370 (w), 1260 (br, w), 1164 (w), 1014 (s), 825 (br, w) cm^{-1}. MS: 119 (45.8%), 120 (74.5%), 121 (96.1%), 122 (100.0%), 123 (79.7%), 124 (50.7%), 125 (28.8%), 126 (10.6%), 127 (2.9%), 128 (1.1%).

1-d_7: prepared according to the procedure described above using mesityl-d_7 bromide. ^{1}H NMR (THF-d_8): 130.0 (s), 104.3 (s, *p*-CHD_2), 103.9 (s, *p*-CH_2D), 103.4 (s, *p*-CH_3, assignments based on integrated peak area and comparison to mesityl-d_7 bromide, see above), 3.59 (m, THF), 1.74 (m, THF), −20.6 (br s). IR (Nujol): 2140 (br, w), 1580 (w), 1250 (br, w), 1035 (s), 910 (sh, m), 880 (s), 670 (br, w) cm^{-1}.

2-d_7: prepared according to the procedure described above starting with **1-d_7**. ^{1}H NMR (toluene-d_8): 15.11 (s), 10.99 (s), 9.66 (s) and 9.63 s) (the resonance at 9.66 ppm has a downfield shoulder, presumably caused by the CHD_2 group), 8.02 (s), 2.07 ns), −20.74 (m, see Figure 4b) ppm. IR (Nujol): 2140 (br, w), 1580 (s), 1290 (m), 1250 (m), 1020 (br, w), 820 (br, w) cm^{-1}.

1-Bromo-2,4,6-tris(monodeuteriomethyl)benzene (Mesityl-d_3 Bromide). 1,3,5-Benzenetricarboxylic acid was converted into the methyl ester by Clinton's method.[31] This was reduced to 1,3,5-tris(hydroxymethyl)benzene by reduction with $LiAlH_4$ and converted into 1,3,5-tris(chloromethyl)benzene with thionyl chloride as described by Storck et al.[32] A solution of 8.4 g of the trichloride (0.038 mol) in 25 mL of THF was slowly added to a solution of 2.5 g of $LiAlD_4$ (98 atom %) in 50 mL of THF. The mixture was heated to reflux for 1 h. After the mixture was cooled to room temperature, 2.4 mL of H_2O, 2.4 mL of 15% KOH, and another 7.2 mL of H_2O were added. The suspension was filtered, and the solids were extracted with boiling THF. Standard workup and distillation yielded 2.5 g of 1,3,5-tris(monodeuteriomethyl)benzene (0.020 mol, 54% yield). ^{1}H NMR ($CDCl_3$): 6.85 (s, 3 H), 2.32 (t, 6 H). IR (neat): 2990 (s), 2905 (s), 2165 (m), 1605 (s), 1460 (m), 1270 (br, w), 990 (br, w), 850 (br, m), 805 (m), 680 (s) cm^{-1}. Mesitylene-d_3 was converted to the bromide by the procedure described above for mesitylene-d_7 (2.52 g, 62% yield). ^{1}H NMR ($CDCl_3$): 6.88 (s, 2 H), 2.36 (t, 4 H, J_{HD} = 2.2 Hz), 2.22 (t, 2 H, J_{HD} = 2.2 Hz) ppm. IR (neat): 3000 (w), 2940 (m), 2900 (s), 2170 (w), 1580 (w), 1450 (s), 1272 (w), 1250 (w), 1164 (w), 1100 (br, w), 1017 (s), 830 (br, w), 680 (w) cm^{-1}.

1-d_9: prepared according to the procedure described above using mesityl-d_3 bromide. ^{1}H NMR (THF-d_8): 129.9 (s, 2 H), 103.3 (s, 2 H), 3.57 (m, THF), 1.74 (m, THF), −20.1 (br s, 4 H) ppm. IR (Nujol): 2160 (w), 1480 (w), 1260 (w), 1040 (s), 910 (w), 885 (m), 810 (w) cm^{-1}.

2-d_{12}: prepared according to the procedure described above using **1-d_9**. ^{1}H NMR (toluene-d_8): 15.2 (s, 2 H), 11.1 (s, 2 H), 9.8 (s, 2 H), 8.0 (s, 2 H), 2.1 (s, 4 H), −20.7 (s, 4 H) ppm.

Preparation of 2 from a Mixture of 1 and 1-d_9. A 1:1 mixture of **1** and **1-d_9** was treated with HBF_4·Et_2O as described above and 54 mg of a mixture of dimers isolated. ^{1}H NMR (toluene-d_8): 15.13 (t), 11.00 (t), 9.70 (s, p-CH_2D), and 9.67 (s, p-CH_3, assignments based on integrals), 8.00 (s), 2.11 (m), −20.7 (m) ppm (see Figure 4c for upfield multiplet and supplementary material for downfield part of spectrum).

Magnetic Measurements. Measurements of magnetic susceptibilities in the temperature range 2–300 K were performed on polycrystalline samples by using a Faraday balance. Variable-temperature control was obtained by using a helium flow cryostat. Samples were loaded into high purity quartz buckets in a drybox and transferred to the cryostat in an O-ring sealed container (for **1**) or sealed in a short quartz tube under helium (for **2**). Typical sample sizes were (10–20) ± 0.1 mg (weighed in the balance at zero field). The diamagnetic force due to the sample holder was subtracted over the entire temperature range. The sample of **1** was measured at full field and 70% of full field to

(30) Smith, L. I. In *Organic Syntheses*; Wiley: New York, 1943; Coll. Vol. II, p 97.
(31) Clinton, R. O.; Laskowsky, S. C. *J. Am. Chem. Soc.* **1984**, *70*, 3135.
(32) Storck, W.; Manecke, G. *Makromol. Chem.* **1975**, *176*, 97.

Table IV. Crystal Data for 2

formula	$C_{36}H_{44}Co_2$
fw	594.61
cryst system	triclinic
space group	$P\bar{1}$
Z	4
a, Å	12.598 (7)
b, Å	16.046 (8)
c, Å	16.855 (6)
α, deg	67.63 (4)
β, deg	87.85 (4)
γ, deg	84.65 (4)
V, Å^3	3137 (3)
d_{calcd}, g/cm^3	1.259
cryst dimens, mm	0.5 × 0.5 × 0.3
diffractometer	Syntex $P2_1$
radiatn	Mo Kα (λ = 0.71073 Å)
temp, K	203
scan method	2θ–θ
2θ range, deg	0–50
scan rate, deg/min	variable, 5–30
no. of data collected	10030
no. of unique data > 6σ	7311
no. of parameters refined	687
absn coeff, mm^{-1}	1.076
R	0.063
R_w	0.084

Table V. Extended Hückel Parameters

atom	orbital	H_{ii}, eV	ζ_1	ζ_2[a]	C_1	C_2[a]
Co	4s	−9.21	2.0			
	4p	−5.29	2.0			
	3d	−13.18	5.55	2.1	0.5678	0.6059
C	2s	−21.4	1.625			
	2p	−11.4	1.625			
H	1s	−13.6	1.30			

[a] ζ_2 and C_2 are the exponent and coefficient used in the double ζ expansion.

check for ferromagnetic impurities (no significant deviations were found). The data were fitted with a Curie–Weiss expression ($\chi_m = C/(T-\Theta)$ + TIP; C = 1.79 emu·K/mol, Θ = 2.8 K, TIP = 1.04 × 10^{-3} emu/mol). The room temperature moment of 3.80 μ_B is corrected for diamagnetism and TIP. **2** was measured at 70% of full field only, and the sample was checked for ferromagnetic impurities by the method of Honda and Owen.[33] The ferromagnetic contribution to the susceptibility was negligible, <1.5%).

(33) Bates, L. F. *Modern Magnetism*, 3rd ed.; Cambridge University Press: Cambridge, 1951; p 133.

Calibration was performed with $HgCo(SCN)_4$ (16.44 × 10^{-6} emu/g at 298 K). All data were corrected for diamagnetism by using Pascal constants[34] (−493 × 10^{-6} emu/mol for **1** and −251 × 10^{-6} emu/mol for **2**).

X-ray Structure Determination of 2. A single crystal of **2** was obtained by cooling a pentane solution to −35 °C. This was sealed in a glass capillary under N_2. Crystal data and a summary of parameters pertinent to the data collection are given in Table IV. All crystallographic calculations were performed on a Prime 9950 computer operated by the Cornell Chemistry Computing Facility. Principal programs employed were as follows: RANTAN 80 and MULTAN 78 (locally modified to perform all Fourier calculations) by P. Main, S. E. Hull, L. Lessinger, G. Germain, J. P. Declercq, and M. M. Woolfson, University of York, England, 1980; BLS 78A, by K. Hirotsu and E. Arnold, Cornell University, 1980; REDUCE and UNIQUE, data reduction programs, by M. E. Lewonowicz, Cornell University, 1978; PL1PLOT, by G. VanDuyne, Cornell University, 1984; and TABLES, by G. VanDuyne, Cornell University, 1986.

MO Calculations. The calculations used the extended Hückel Hamiltonian and the weighted H_{ij} formula.[35] Parameters are listed in Table V and were taken from the literature. The geometry used was an idealized D_{2h} model of the experimental structure with Co–Co, Co–C, C–H, and C–C distances of 2.57, 1.80, 1.09, and 1.41 A, respectively.

Acknowledgment. This research was supported by grants from Research Corp., the National Science Foundation (CHE-8451670 and CHE-8512710), NATO (Collaborative Research Grant No. 86/0449), the Camille and Henry Dreyfus Foundation, the Atlantic Richfield Foundation, Dow Chemical Co., Rohm and Haas Co., and Cornell University.

Registry No. **1**, 121425-60-3; **1**-d_9, 121425-65-8; **1**-$D_?$, 121425-63-6; **2**, 121471-30-5; **2**-d_{12}, 121440-70-8; **2**-$d_?$, 121471-31-6; $[PPN]^+[(Co(mesityl)_3]^-$, 121425-61-4; $CoCl_2$, 7646-79-9; PPN^+Cl^-, 21050-13-5; mesityl bromide, 576-83-0; mesityl-$d_?$ bromide, 121425-57-8; mesityl-d_3 bromide, 121425-58-9; mesitylene, 108-67-8; 1-bromo-2,4,6-tris(chloromethyl)benzene, 17299-97-7.

Supplementary Material Available: Tables of anisotropic thermal parameters, hydrogen atom positions for **2** and the ^1H NMR spectrum of **2** prepared from **1**-d_0 and **1**-d_9 (8 pages); a listing of observed and calculated structure factors (34 pages). Ordering information is given on any current masthead page.

(34) Koenig, E.; Koenig, G. *Landolt-Boernstein, Neue Serie, II*; Springer: Berlin, 1976; Vol. 8, pp 27–29.

(35) Ammeter, J. H.; Buergi, H.-B.; Thibeault, J. C.; Hoffmann, R. *J. Am. Chem. Soc.* **1978**, *100*, 3686.